Available online at www.sciencedirect.com
SCIENCE DIRECT®
Journal of Sound and Vibration 280 (2005) 759–775
JOURNAL OF SOUND AND VIBRATION
www.elsevier.com/locate/jsvi

Robust control of a hydraulically driven flexible arm using backstepping technique

Guang Li[a], Amir Khajepour[b,*]

[a]*Department of Mechanical Engineering, Zhuzhou Institute of Technology, Zhuzhou, China*
[b]*Department of Mechanical Engineering, University of Waterloo, Waterloo, Ont., Canada N2L 3G1*

Received 19 August 2002; accepted 17 December 2003
Available online 23 September 2004

Abstract

In this paper, a new robust controller is proposed to regulate both flexural vibrations and rigid body motion of a hydraulically driven flexible arm. The proposed controller combines backstepping, sliding mode, and pole placement techniques to arrive at a controller capable of dealing with a nonlinear system with uncertainties. The sliding mode technique is used to achieve an asymptotic joint angle and vibration regulation in the presence of payload uncertainty by providing a virtual torque input at the joint while the backstepping technique is used to regulate the spool position of a hydraulic valve to provide the required torque. The pole placement design methodology is applied to attain a good dynamic response by placing the poles of the sliding plane in the desired location. It is shown that in contrary to conventional use of sliding mode controllers, there is no chatter in the hydraulic valve which results in smoother and noiseless operation of the system.

1. Introduction

One of the major obstacles that limits fast manipulation of hydraulic cranes or lightweight robotic devices is inherent flexibility of the structure and/or hydraulic actuators. To achieve higher stiffness, the members of the system structure have to be rigid which in turn increases inertia and

*Corresponding author. Tel.: +1-519-888-4567x6159; fax: +1-519-888-6197.
E-mail address: akhajepour@uwaterloo.ca (A. Khajepour).

0022-460X/$ - see front matter © 2004 Elsevier Ltd. All rights reserved.
doi:10.1016/j.jsv.2003.12.055

requires large actuation power. As a result, lightweight structures with special controllers are needed for high speed manipulators.

The problem of controlling the position of a flexible manipulator while minimizing link flexural vibration has received considerable attention in recent years, and different approaches have been investigated. The work by Book and co-workers represents one of the earliest studies in the control of flexible manipulators [1]. They linearized the equations of motion about a nominal configuration and applied several linear control schemes to control flexible manipulator arms. Linear control methods were also applied by Cannon et al. [2,3]. A variety of other control strategies have also been proposed. Meckl and Seering [4] proposed shaped torque techniques to minimize the residual vibrations in flexible manipulators. This technique has been developed further to suppress multiple mode oscillations [5].

The computed torque method [6] which was originally developed for rigid manipulators was also tried on flexible link systems. The complexity of inverse dynamics makes a straightforward application of the computed torque method or feedback linearization impossible; instead, some approximation schemes were proposed for open and closed-loop control [7,8]. Oakley and Cannon [9] performed some experiments on the performance of independent joint PD control of a two-link rigid-flexible manipulator. The sliding mode control, because of its robustness and simplicity, has been applied to the control of rigid and flexible robot manipulators [10]. Several artificial intelligence control methods also have been applied to flexible manipulators. Kubica and Wang [11] developed a fuzzy control strategy for a flexible link arm, while Cheng and Wen [12] proposed a neural network controller for flexible-link robots.

There are few studies of controlling hydraulically driven flexible manipulators. The complex dynamics of this kind of control problem consists of the interaction of rigid body motion, beam flexural vibration, and hydraulic actuator dynamics. Panza and Mayne [13,14] presented the theoretical and experimental investigation of controlling a rotating flexible beam driven by a hydraulic actuator. Their control was based on simple position feedback, along with a hydraulic actuation system tuned to suppress beam vibration over a range of angular motion. The load-compensated feedforward control technique was used by Kwon et al. [15] for the tracking control of a flexible manipulator.

The control techniques (except the sliding mode control) mentioned above are not robust when regulating the tip position of a flexible manipulator in the presence of an unknown payload and parameter uncertainties such as stiffness, oil bulk modulus, leakages, etc. Although the sliding mode control is robust, the chattering in the hydraulic valve spool resulting from the control technique is detrimental to the hydraulic system and may induce higher vibrational modes in the system.

This paper studies the robust position control of a large-size hydraulically actuated flexible manipulator (a version of an industrial crane). A controller which utilizes backstepping [16], sliding mode, and pole placement techniques is proposed. The general approach to design the robust controller is: (1) the sliding mode technique is applied to achieve a virtual input torque to the flexible arm system in the presence of payload uncertainties, (2) the pole placement is used to attain a good transient performance by tuning the poles of the sliding plane, and (3) the backstepping technique is adopted to attain the system actual input, namely the displacement of a hydraulic valve spool to achieve the desired joint torque. To investigate the performance of the proposed controller, numerical simulations are presented. It is shown that the proposed controller

does not result in any chatter in the hydraulic valve which is the consequence of conventional use of sliding mode controllers.

2. Dynamic formulation and problem statement

A hydraulically driven single-link flexible arm is shown in Fig. 1. l is the length of the arm and l_0, l_1, α specify the location and orientation of the hydraulic actuator. There are two coordinates: the inertial frame XOY and link-fixed frame x_1Oy_1. The coordinate frame x_1Oy_1 is attached to the arm with x_1 in the direction of the un-deformed arm. The angle between Ox_1 and OX of the inertial frame is shown by θ. The deflection of the arm from its rigid body motion is indicated by $w(x,t)$. The mass of the arm and the concentrated tip payload are denoted by m and m_p, respectively. The overall length of the hydraulic actuator and its force applied to the arm are denoted by y and F, respectively. The normal component of F to the arm is shown by F' in Fig. 1b.

2.1. Elastic deflection of the arm

In the modeling of the flexible arm, the transverse shear and rotary inertia effects are neglected because the arm is assumed to be long and slender. This allows the use of the Bernoulli–Euler beam theory to model the elastic behavior of the arm. Also, the arm is assumed to be stiff in the plane normal to XOY and thus, the dominant vibration occurs in one plane (XOY). Moreover, the arm is considered to have a constant cross-section with uniform material properties throughout.

Using the assumed-mode method, the elastic deflection of the manipulator can be described as

$$w(x,t) = \sum_{i=1}^{n} \phi_i(x) q_i(t), \tag{1}$$

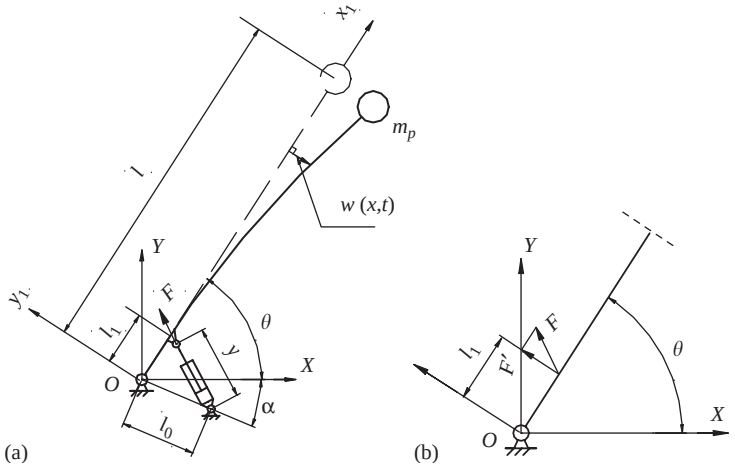

Fig. 1. (a) Schematic of the flexible arm; (b) actuator force.

where $\phi_i(x)$ and $q_i(t)$ denote modal shape functions and modal coordinates, respectively, and n is the number of modes used in the computation.

2.2. Dynamic model for the flexible arm

Referring to Fig. 1 and by using appropriate orthogonal conditions on the mode functions, the kinetic (T) and potential (V) energy of the arm can be determined as [17,18]

$$T = \tfrac{1}{2}\dot{\theta}^2 J + \frac{m}{2l}\sum_{i=1}^{n} A_i \dot{q}_i^2 + \frac{m}{2l}\dot{\theta}^2 \sum_{i=1}^{n} A_i \dot{q}_i^2 + \frac{m}{l}\dot{\theta}\sum_{i=1}^{n} B_i \dot{q}_i + \frac{m_p}{2}\left(l^2\dot{\theta}^2 + \sum_{i=1}^{n} C_i^2 \dot{q}_i^2 + \dot{\theta}^2 \sum_{i=1}^{n} C_i^2 \dot{q}_i^2 + 2l\dot{\theta}\sum_{i=1}^{n} C_i \dot{q}_i\right), \tag{2}$$

$$V = \tfrac{1}{2} mgl \sin\theta + \frac{EI}{2}\sum_{i=1}^{n} D_i q_i^2,$$

where

$$A_i = \int_0^l \phi_i^2(x)\,\mathrm{d}x, \quad B_i = \int_0^l x\phi_i(x)\,\mathrm{d}x,$$
$$C_i = \phi_i(l), \quad D_i = \int_0^l \left[\frac{\mathrm{d}^2\phi_i(x)}{\mathrm{d}x^2}\right]^2 \mathrm{d}x. \tag{3}$$

In Eq. (2), J is the arm's moment inertia about its joint axis O, and EI the arm's flexural rigidity. Note that the effect of flexure on the potential energy has been ignored.

Applying the Lagrange's method, the equations of motion are obtained as

$$\frac{\mathrm{d}}{\mathrm{d}t}\left[\frac{\partial T}{\partial \dot{q}_j}\right] - \frac{\partial T}{\partial q_j} + \frac{\partial V}{\partial q_j} = R_j, \quad j = 0, 1, \ldots, n, \tag{4}$$

where q_j is the generalized coordinate, $q = [\theta\ q_1 \ldots q_n]^{\mathrm{T}}$, and R_j is the generalized force corresponding to the generalized coordinate q_j. The generalized forces are determined from the virtual work δW for the hydraulic actuator force F acting on the arm at a distance l_1 from the base as shown in Fig. 1(b).

For the first generalized coordinate θ, the virtual work for a virtual change is

$$\delta W_0 = F\,\delta y, \tag{5}$$

where δy is the displacement vector of the actuator due to $\delta\theta$. The generalized force is then

$$R_0 = \frac{\partial W_0}{\partial \theta}, = F\frac{\partial y}{\partial \theta} = T_f, \tag{6}$$

where T_f denotes the resultant torque of the hydraulic actuator force F on the arm. The remaining generalized forces are

$$R_j = 0, \quad j = 1, 2, \ldots, n. \tag{7}$$

It should be noted that y does not introduce a new variable and as seen in the Fig. 1(a)

$$y = \sqrt{l_1^2 + l_0^2 - 2l_1 l_0 \cos(\theta + \alpha)}. \tag{8}$$

For the elastic deflection of the arm in Eq. (1), it has been shown in Ref. [19] that using the first mode of vibration provides a satisfactory response. As a result, we shall consider only the first flexural mode of the arm for the beam deflection, i.e., Eq. (1) becomes

$$w(x, t) = \phi_1(x) q_1(t). \tag{9}$$

Since it is assumed that the beam's length l is much greater than l_1 (actuator connection), the modes of a clamped–free beam can be considered in Eq. (9). This mode is [18]

$$\phi_1(x) = \sin(\beta_1 x) - \sinh(\beta_1 x) - \frac{\sin \beta_1 l + \sinh \beta_1 l}{\cos \beta_1 l + \cosh \beta_1 l} (\cos(\beta_1 x) - \cosh(\beta_1 x)), \tag{10}$$

where $\beta_1 l = 1.875$.

Using Eq. (4) along with Eqs. (2) and (3), the dynamic equations of the system can be described as

$$M \begin{bmatrix} \ddot{\theta} \\ \ddot{q}_1 \end{bmatrix} + \begin{bmatrix} v_0 \\ v_1 \end{bmatrix} = \begin{bmatrix} T_f \\ 0 \end{bmatrix}, \tag{11}$$

where

$$M = \begin{bmatrix} \alpha_0 & \gamma_1 \\ \gamma_1 & \alpha_1 \end{bmatrix} = \begin{bmatrix} J + m_p l^2 + \dfrac{m}{l} A_1 q_1^2 + m_p C_1^2 q_1^2 & \dfrac{m}{l} B_1 + m_p l C_1 \\ \dfrac{m}{l} B_1 + m_p l C_1 & \dfrac{m}{l} A_1 + m_p C_1^2 \end{bmatrix}, \tag{12}$$

$$\begin{bmatrix} v_0 \\ v_1 \end{bmatrix} = \begin{bmatrix} 2\dot{\theta}\dot{q}_1 q_1 \left(\dfrac{m}{l} A_1 + m_p C_1^2\right) + \dfrac{1}{2} mg \cos \theta \\ \mathrm{EI} D_1 q_1 - \dot{\theta}^2 q_1 \left(\dfrac{m}{l} A_1 + m_p C_1^2\right) \end{bmatrix}. \tag{13}$$

In the following we study the dynamics of the hydraulic actuator and valve to obtain the torque T_f in Eq. (11).

2.3. Dynamic model of the hydraulic actuator and valve

The schematic of the hydraulic servo system driving the flexible manipulator is depicted in Fig. 2. P_1 and P_2 (res. Q_1 and Q_2) are the forward and return pressures (res. flow rates) of the hydraulic cylinder. The supply pressure of the pump is shown by P_s, and P_r is the tank reference pressure.

Assuming that the time constant of the servo valve motor/flapper is much smaller than those of the mechanical parts, we can consider the spool displacement x_v as the control input. The flow

rates Q_1 and Q_2 are

$$Q_1 = k_q g_1(P_1, \text{sign}(x_v))x_v, \quad Q_2 = k_q g_2(P_2, \text{sign}(x_v))x_v, \tag{14}$$

where

$$g_1(P_1, \text{sign}(x_v)) = \begin{cases} \sqrt{P_s - P_1}, & x_v \geqslant 0, \\ \sqrt{P_1 - P_s}, & x_v < 0, \end{cases}$$
$$g_2(P_2, \text{sign}(x_v)) = \begin{cases} \sqrt{P_2 - P_r}, & x_v \geqslant 0, \\ \sqrt{P_s - P_2}, & x_v < 0 \end{cases} \tag{15}$$

and k_q is the flow gain coefficient of the servo valve.

Applying the flow continuity equations to the two sides of the cylinder and neglecting any external leakage [20]

$$Q_1 = A_1 \frac{\mathrm{d}y}{\mathrm{d}t} + \frac{V_1}{\beta_e}\dot{P}_1 + C_{tm}(P_1 - P_2),$$
$$Q_2 = A_2 \frac{\mathrm{d}y}{\mathrm{d}t} - \frac{V_2}{\beta_e}\dot{P}_2 + C_{tm}(P_1 - P_2), \tag{16}$$

where β_e is the effective bulk modulus, V_1 and V_2 are the volumes of the cylinder's chambers and C_{tm} is the coefficient of the internal leakage of the cylinder. It should be noted that V_1 and V_2 are functions of y and using Eq. (8) they can be expressed as functions of θ. Solving for $\dot{P}_1$ and $\dot{P}_2$ in Eq. (16), the dynamics of the cylinder and its valve can be written as

$$\dot{P}_1 = \frac{\beta_e}{V_1(\theta)}\left(Q_1 - A_1 \frac{\partial y}{\partial \theta}\dot{\theta} - C_{tm}(P_1 - P_2)\right), \tag{17}$$

$$\dot{P}_2 = \frac{\beta_e}{V_2(\theta)}\left(A_2 \frac{\partial y}{\partial \theta}\dot{\theta} + C_{tm}(P_1 - P_2) - Q_2\right). \tag{18}$$

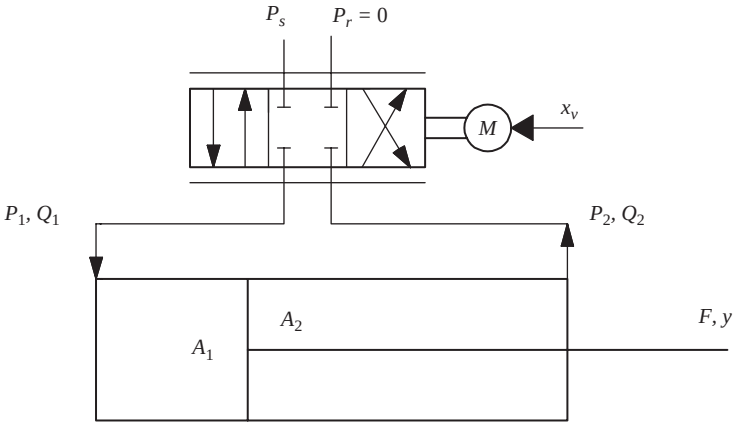

Fig. 2. Hydraulic servo system.

The force that is applied by the actuator to the arm is simply

$$F = P_1 A_1 - P_2 A_2, \tag{19}$$

where using Eq. (6) the torque on the arm can be calculated.

In the following, we develop a robust controller to control and regulate both the rigid body motion and the oscillation of the flexible arm. The task of the controller is to regulate the position of the servo valve's spool so that the joint angular displacement θ asymptotically approaches the desired angle as close as possible, while the manipulator deflections and vibrations remain as small as possible.

3. Controller design

The backstepping design methodology has become increasingly popular in nonlinear control systems. The main idea of this technique is to design a controller recursively by considering some of the state variables as "virtual controls". Here, we summarize the method and implement the technique to the flexible arm.

Consider that the equations of a system are represented in the form

$$\dot{x} = f(x) + g(x)\xi, \tag{20a}$$

$$\dot{\xi} = u, \tag{20b}$$

where $x \in \Re^n$, and $\xi \in \Re$ are the state variables. To stabilize system of Eq. (20), we assume that ξ is a virtual control input for Eq. (20a) and there exists a feedback control law for its stabilization. If we consider the virtual input as $\xi = \alpha(x)$ and an unbounded function $V(x)$ such that

$$\frac{\partial V}{\partial x}(f(x) + g(x)\alpha(x)) \leqslant -W(x) \leqslant 0. \tag{21}$$

Eq. (20a) is globally asymptotically stable for $x = 0$ if $W(x)$ is positive definite.

To stabilize the overall system of Eq. (20), we assume

$$V_a(x) = V(x) + \tfrac{1}{2}(\xi - \alpha(x))^2 \tag{22}$$

as a control Lyapunov function (CLF). In Ref. [16], it is shown that there exists a feedback control $u(x, \xi)$, which renders $x = 0,\ \xi - \alpha(x) = 0$ as a globally asymptotically stable equilibrium of Eq. (20). Furthermore, if $W(x)$ is only positive semi-definite, then there exists a feedback control law which guarantees global boundedness and convergence of $(x(t)\ \xi(t))$ to the largest invariant set of Eq. (20). For a more comprehension discussion of the backstepping technique please refer to Ref. [16].

The equations of the flexible arm developed in the previous section can be presented in the form shown in Eq. (20) as the cascade of two parts: the flexible arm dynamics Eq. (11), and the hydraulic actuator dynamics Eqs. (17) and (18). According to this arrangement, the arm dynamics Eq. (11) are controlled by torque T_f applied by the hydraulic actuator, and the actuator dynamics are controlled by the servo valve spool displacement x_v (the actual control input). As seen in Fig. 3, the desired rigid angle of the link θ_d when compared with the actual angle θ, and the sliding mode controller generates the virtual control input T_v. To generate this torque by the hydraulic

actuator, the spool displacement x_v must be controlled. This is done by the backstepping controller for the dynamics of the hydraulic valve.

To find a feedback control law to stabilize and control the flexible arm, we assume $T_v = T_f$ as a virtual control input and ignore the "backstepping controller" and "hydraulic dynamics" blocks in Fig. 3 and use the sliding mode control to arrive at a control law for T_v. To stabilize and control the arm assuming T_v as the virtual control input, any control technique can be used. However, we use the sliding mode control since it is a powerful control approach capable of providing robust performance for nonlinear systems with uncertainties. In the following, the details of the controller design are discussed.

3.1. Hybrid sliding mode and backstepping controller design

In this paper, for simplicity, we consider the parametric uncertainties due to the unknown tip payload m_p and oil bulk modulus β_e. Other parametric uncertainties can be dealt with in the same way if necessary.

Step 1: Rewrite the equations of flexible arm Eq. (11), and replace the torque T_f by the virtual control input T_v

$$\dot{x} = f(x) + g(x)T_v, \tag{23}$$

where

$$x = [x_1\ x_2\ x_3\ x_4]^{\mathrm{T}} = [\theta\ q_1\ \dot{\theta}\ \dot{q}_1]^{\mathrm{T}},$$

$$f(x) = \left[x_3\ \ x_4\ \ \left(-M^{-1} \begin{bmatrix} v_0 \\ v_1 \end{bmatrix} \right)^{\mathrm{T}} \right]^{\mathrm{T}},$$

$$g(x) = \left[0\ \ 0\ \ \left(M^{-1} \begin{bmatrix} 1 \\ 0 \end{bmatrix} \right)^{\mathrm{T}} \right]^{\mathrm{T}}.$$

To obtain the virtual control input T_v using the sliding mode method, the error e is defined as

$$e = x - x_d, \tag{24}$$

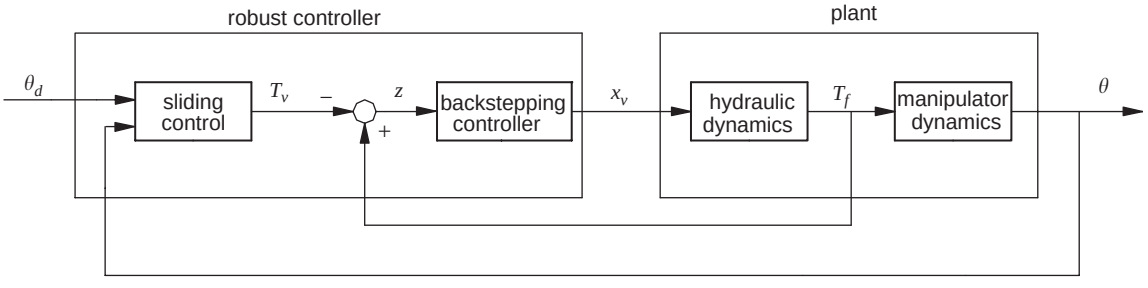

Fig. 3. General structure of the proposed controller.

where x_d is the desired state of the system. The sliding plane s can be defined as

$$s = \lambda^{\mathrm{T}} e, \quad \lambda = [\lambda_1 \ 1 \ \lambda_2 \ \lambda_3]^{\mathrm{T}}, \tag{25}$$

where λ_1, λ_2 and λ_3 are constants which will be determined using the pole placement technique to ensure a satisfactory response for the closed-loop system of Eq. (23) [10]. In the sliding mode method, the control input T_v is selected such that the trajectories near the sliding surface directed toward the surface. When the system is on the surface, its dynamics is governed by the equation of the surface. To determine the input T_v, we assume

$$T_v = T_{su} + T_s, \tag{26}$$

where T_{su} is for keeping the system on the surface and T_s is for directing the trajectories towards the surface. Therefore, T_s must be zero on the surface. When the system is on the surface, we have

$$s = 0 \quad \text{and} \quad \dot{s} = 0 \tag{27}$$

and hence, assuming $\dot{x}_d = 0$,

$$\dot{s} = \lambda^{\mathrm{T}} \dot{e} = \lambda^{\mathrm{T}} \dot{x} \tag{28}$$

Substituting from Eq. (23), Eq. (28) becomes

$$\dot{s} = \lambda^{\mathrm{T}}(f(x) + g(x)T_{su}). \tag{29}$$

Solving for T_{su}, and assuming nominal values for the parameters, yields

$$T_{su} = -\frac{\lambda^{\mathrm{T}} \hat{f}(x)}{\lambda^{\mathrm{T}} \hat{g}(x)}, \tag{30}$$

where $\hat{f}(x)$ and $\hat{g}(x)$ represent $f(x)$ and $g(x)$ calculated at the nominal values of the parameters.

Now to calculate T_s, we use a Lyapunov function V and choose $T_v = T_{su} + T_s$ such that $\dot{V}$ negative definite. The Lyapunov candidate function is considered as

$$V = \tfrac{1}{2} s^2, \tag{31}$$

where its time derivative is

$$\begin{aligned} \dot{V} &= s\dot{s}, \\ &= s\lambda^{\mathrm{T}}(f(x) + g(x)(T_{su} + T_s)) \\ &= s(\lambda^{\mathrm{T}}(f(x) + g(x))T_{su} + \lambda^{\mathrm{T}} g(x) T_s). \end{aligned} \tag{32}$$

It was shown in Eq. (29) that $\lambda^{\mathrm{T}}(f(x) + g(x))T_{su}$ is zero if there are no uncertainties in the parameters. However, assuming that the uncertainties are bounded, it is shown in Ref. [21] that by assuming

$$T_s = -k \operatorname{sign}(s) \tag{33}$$

there exists a positive switching gain k such that $\dot{V}$ in Eq. (32) becomes negative definite which guarantees the stability of the system. Eq. (32) using Eqs. (30) and (33) can be written as [21]

$$\frac{\mathrm{d}}{\mathrm{d}t}\left(\tfrac{1}{2} s^2\right) = s\dot{s} \leqslant -\eta |s|, \tag{34}$$

where η is a positive constant.

Step 2: Introducing z as a new variable defined by

$$z = T_f - T_v \tag{35}$$

with the system of the arm's equations (11), $\dot{z}$ can be written as

$$\dot{x} = f(x) + g(x)(T_v + z), \tag{36a}$$

$$\dot{z} = \dot{T}_f - \dot{T}_v, \tag{36b}$$

where $\dot{T}_v$ and $\dot{T}_f$ using Eqs. (36a),(6),(8) and (19) are

$$\dot{T}_v = \left[\frac{\partial T_v}{\partial x}\right]^{\mathrm{T}}, \quad \dot{x} = \left[\frac{\partial T_v}{\partial x}\right]^{\mathrm{T}} (f(x) + g(x)(T_v + z)), \tag{37a}$$

$$\begin{aligned}\dot{T}_f &= \frac{\mathrm{d}}{\mathrm{d}t}\left(F\,\frac{\partial y(x_1)}{\partial x_1}\right)\\ &= \frac{\mathrm{d}}{\mathrm{d}t}\left((P_1A_1 - P_2A_2)\frac{\partial y(x_1)}{\partial x_1}\right)\\ &= (\dot{P}_1A_1 - \dot{P}_2A_2)\frac{\partial y(x_1)}{\partial x_1} + (P_1A_1 - P_2A_2)\frac{\partial y^2(x_1)}{\partial x_1^2}\,\dot{x}_1.\end{aligned} \tag{37b}$$

Substituting Eqs. (17), (18), and (23) into Eq. (37b) and then into Eq. (36b) $\dot{z}$ becomes

$$\dot{z} = \tau_1(x, P_1, P_2) + \beta_e\tau_2(x, P_1, P_2) + \beta_e x_v\tau_3(x, P_1, P_2) - \left[\frac{\partial T_v}{\partial x}\right]^{\mathrm{T}} (f(x) + g(x)(T_v + z)), \tag{38}$$

where

$$\tau_1(x, P_1, P_2) = \frac{\partial^2 y}{\partial x_1^2}\,x_3(A_1P_1 - A_2P_2),$$

$$\tau_2(x, P_1, P_2) = -\frac{\partial y}{\partial x_1}\left(\frac{A_1}{V_1}\left(A_1\,\frac{\partial y}{\partial x_1}\,x_3 + C_{tm}(P_1 - P_2)\right) + \frac{A_2}{V_2}\left(A_2\,\frac{\partial y}{\partial x_1}\,x_3 + C_{tm}(P_1 - P_2)\right)\right),$$

$$\tau_3(x, P_1, P_2) = \frac{\partial y}{\partial x_1}\left(\frac{A_1}{V_1}\,k_q g_1(P_1, \mathrm{sign}(x_v)) + \frac{A_2}{V_2}\,k_q g_2(P_2, \mathrm{sign}(x_v))\right).$$

Eqs. (17), (18), and (36), with $\dot{z}$ defined in Eq. (38) are the overall equations of the flexible arm with hydraulic actuator. The input of the system is x_v which needs to be defined to control and stabilize the system. To obtain x_v, a control Lyapunov function is chosen as

$$V_a(x, P_1, P_2, x_v) = \tfrac{1}{2}s^2 + \tfrac{1}{2}z^2, \tag{39}$$

where its derivative is

$$\begin{aligned}\dot{V}_a &= s\dot{s} + z\dot{z}\\ &= s[\lambda^{\mathrm{T}}(f(x) + g(x)T_v)]\\ &\quad + z\left[\tau_1 + \beta_e\tau_2 + \beta_e x_v\tau_3 + s\lambda^{\mathrm{T}}g(x) - \left[\frac{\partial T_v}{\partial x}\right]^{\mathrm{T}}(f(x) + g(x)T_v) - \left[\frac{\partial T_v}{\partial x}\right]^{\mathrm{T}} g(x)z\right]. \end{aligned} \tag{40}$$

Reconsidering the flexible arm equation (23), and neglecting small quadratic term x_3^2, i.e., q_1^2, it can be rewritten as

$$\dot{x} = (\hat{f}(x) + \phi_1(x)\Delta_f) + (\hat{g}(x) + \phi_2(x)\Delta_g)T_v, \tag{41}$$

where $\varphi_1(x)$ and $\varphi_2(X)$ are (4×4) matrices of known nonlinear functions, and Δ_f and Δ_g are (4×1) error vectors between actual and nominal values for the uncertain parameters. Substituting Eqs. (34) and (41) into Eq. (40) results in

$$\begin{aligned}\dot{V}_a \leqslant & -\eta|s| + z\left[\tau_1 + s\lambda^{\mathrm{T}}\hat{g}(x) - \left[\frac{\partial T_v}{\partial x}\right]^{\mathrm{T}}(\hat{f}(x) + \hat{g}(x)T_v) - \left[\frac{\partial T_v}{\partial x}\right]^{\mathrm{T}} g(x)z\right]\\ &+ z\left[\beta_e\tau_2 + \beta_e x_v\tau_3 + s\lambda^{\mathrm{T}}\phi_2(x)\Delta_g - \left[\frac{\partial T_v}{\partial x}\right]^{\mathrm{T}}(\phi_1(x)\Delta_f + \phi_2(x)\Delta_g T_v)\right]\\ = & -\eta|s| - \left[\frac{\partial T_v}{\partial x}\right]^{\mathrm{T}}\hat{g}(x)z^2 + \beta_e z\left[\tau_2 + x_v\tau_3 + \chi_1(x)\Delta_1 + \chi_2(x)\Delta_2 + \frac{1}{\hat{\beta}_e}\chi_3 + \chi_3\Delta_3\right], \end{aligned} \tag{42}$$

where $\hat{\beta}_e$ is the nominal value of β_e, and

$$\Delta_1 = \frac{\Delta_f}{\beta_e},$$

$$\Delta_2 = \frac{\Delta_g}{\beta_e},$$

$$\Delta_3 = \frac{1}{\hat{\beta}_e} - \frac{1}{\beta_e},$$

$$\chi_1(x) = -\left[\frac{\partial T_v}{\partial x}\right]^{\mathrm{T}}\phi_1(x),$$

$$\chi_2(x) = -\left[\frac{\partial T_v}{\partial x}\right]^{\mathrm{T}}\phi_2(x)T_v + s\lambda^{\mathrm{T}}\phi_2(x),$$

$$\chi_3(x, P_1, P_2) = \tau_1 + s\lambda^{\mathrm{T}}\hat{g}(x) - \left[\frac{\partial T_v}{\partial x}\right]^{\mathrm{T}}(\hat{f}(x) + \hat{g}(x)T_v).$$

By choosing x_v to be

$$x_v = -\frac{z}{\tau_3}\left[K_1 z + \tau_z + \frac{\chi_3}{\hat{\beta}_e} + \eta_1 z|\chi_1(x)|^2 + \eta_1 z|\chi_2(x)|^2 + \eta_1 z\chi_3^2 - \eta_2 z\right], \tag{43}$$

where K_1 and η_i $(i = 1, 2)$ are positive constants, with η_2 satisfying

$$\beta_{e\,\min}\eta_2 \geqslant \left|\left[\frac{\partial T_v}{\partial x}\right]^{\mathrm{T}} \hat{g}(x)\right|. \tag{44}$$

Substituting Eqs. (43) into Eq. (42), we have

$$\dot{V}_a \leqslant -\eta|s| - Kz^2 + C, \tag{45}$$

where

$$K = \left(\beta_e\eta_2 - \left[\frac{\partial T_v}{\partial x}\right]^{\mathrm{T}} \hat{g}(x)\right) + \beta_e K_1 \geqslant 0,$$

$$C = \beta_e\left[\frac{\|\Delta_1\|_\infty^2 + \|\Delta_2\|_\infty^2 + \Delta_3^2}{4\eta_1}\right] \geqslant 0. \tag{46}$$

The control law (43) guarantees global uniform boundedness of $s(t)$ and $z(t)$ and they converge to the residual set, i.e., $(\theta - \theta_d)$, q_1 with their derivatives exponentially decaying to a ball as $t \to \infty$ [16]. Moreover, the exponential converging rate and the size of the final tracking error can be freely adjusted by the controller gains K and C.

4. Numerical simulation

In order to demonstrate the effectiveness of the proposed robust control strategy, numerical simulations are performed. The flexible beam is constructed from steel which has a rectangular hollow cross-sectional area. In order to reduce the simulation time, a saturation function sat(s) replaces the sign function sign(s) in Eq. (33). This function is described as

$$\mathrm{sat}(s) = \begin{cases} 1, & s > \varepsilon, \\ \dfrac{s}{\varepsilon}, & -\varepsilon \leqslant s \leqslant \varepsilon, \\ -1, & s < \varepsilon, \end{cases} \tag{47}$$

where $\varepsilon > 0$ is the boundary layer width in s. The numerical data of the system are given in Table 1.

For the simulation, we assume that the arm is expected to move from 30° to 60°, and also assume that the nominal values of uncertain parameters are $\hat{m}_p = 400\,\mathrm{kg}$ and $\hat{\beta}_e = 1.5\mathrm{e}9$.

To have a means to evaluate the controller performance, we first simulate the flexible arm assuming a step input for the valve displacement x_v. The valve is opened at $t = 0$ and it is closed when the joint angle of the arm θ reaches 60°. Fig. 4 shows the response of the arm and it can be seen that the joint angle $\theta(t)$ and tip deflection $w(l, t)$ have large oscillations which take more than 5 s to die out.

Table 1
The system parameters used in the simulations

Parameter values	L (m)	l_1 (m)	l_0 (m)	α (°)	EI (Nm^2)	m (kg)	m_p (kg)
Flexible manipulator parameters	10	1	1	0	1.0e8	468	$0 \sim 600$
Parameter values	P_s (N/m^2)	k_q (m)	C_{tm} (m^5/Ns)	ρ (kg/m^3)	A_1 (m^2)	A_2 (m^2)	β_e (N/m^5)
Hydraulic parameters	6e8	0.0063	3e−12	900	0.02	0.01	1e9 $\sim$ 2e9

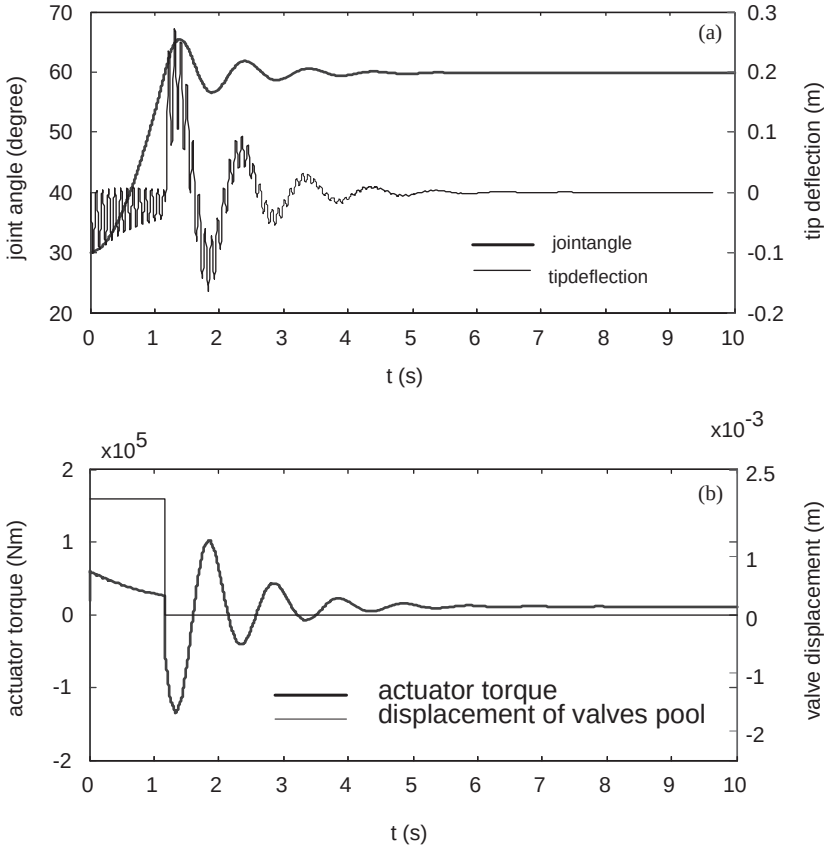

Fig. 4. Simulation results with no controller. (a) Joint angle and tip deflection, (b) torque and displacement of valve spool.

4.1. Pole assignment

As mentioned earlier, the gains of the sliding plane in Eq. (25) are determined by the pole placement approach. To investigate the effects of the poles locations, we choose two cases: case A,

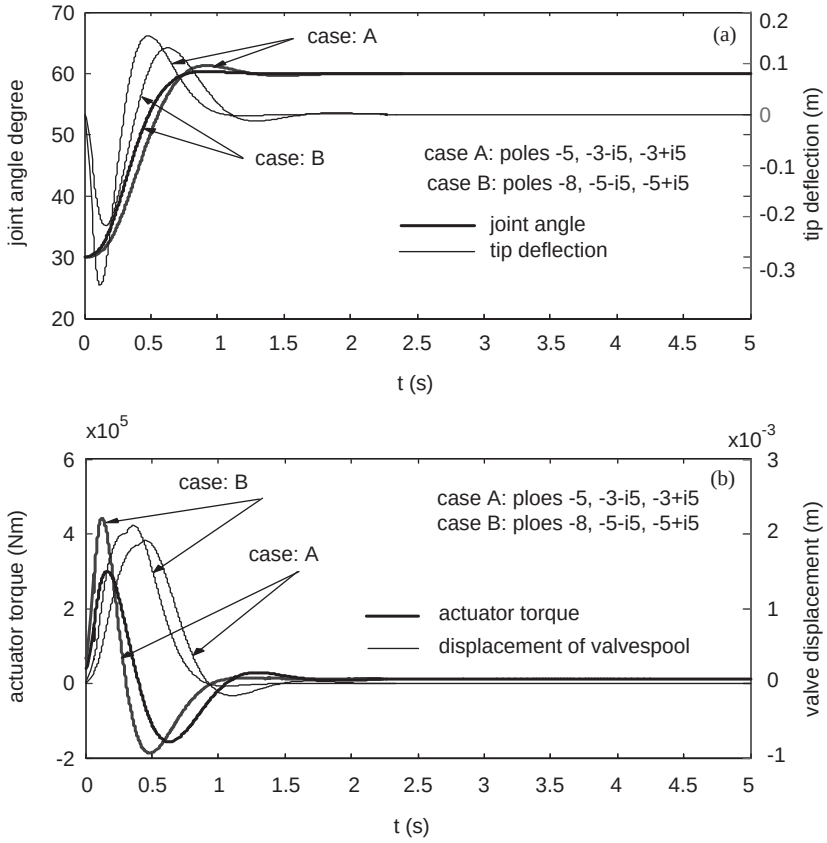

Fig. 5. Simulation results with the proposed controller with different pole assignment. (a) Joint angle and tip deflection, (b) torque and displacement of valve spool.

poles at: -5, $-3 \pm i5$, and case B, poles at: -8, $-5 \pm i5$. Assuming nominal payload ($m_p = 400\,\text{kg}$) the joint angle $\theta(t)$, tip deflection $w(l,t)$, hydraulic actuator torque $T_f(t)$, and the valve spool displacement $x_v(t)$ are plotted in Fig. 5. As expected, case B has a faster response at higher required torque expense. In both the cases, there are no considerable oscillations and in less than 1.5 s the response is settled at the desired location. The spool motion is smooth and there is no chatter in the operation of the valve.

4.2. Robustness

To demonstrate the robustness of the proposed controller to parameters uncertainties, the arm is simulated with the poles of the sliding plane at: $-5, -3 \pm i5$ and system parameters at their extreme values. Fig. 6 shows the response curves of the arm for $m_p = 0$, and 600. As seen in the figure, although the variation in the payload is considerable, however the controller is robust and stabilizes both cases with minimum oscillation and deflection in the arm. Also, there is no chatter in the valve operation as a result of backstepping application in the proposed controller.

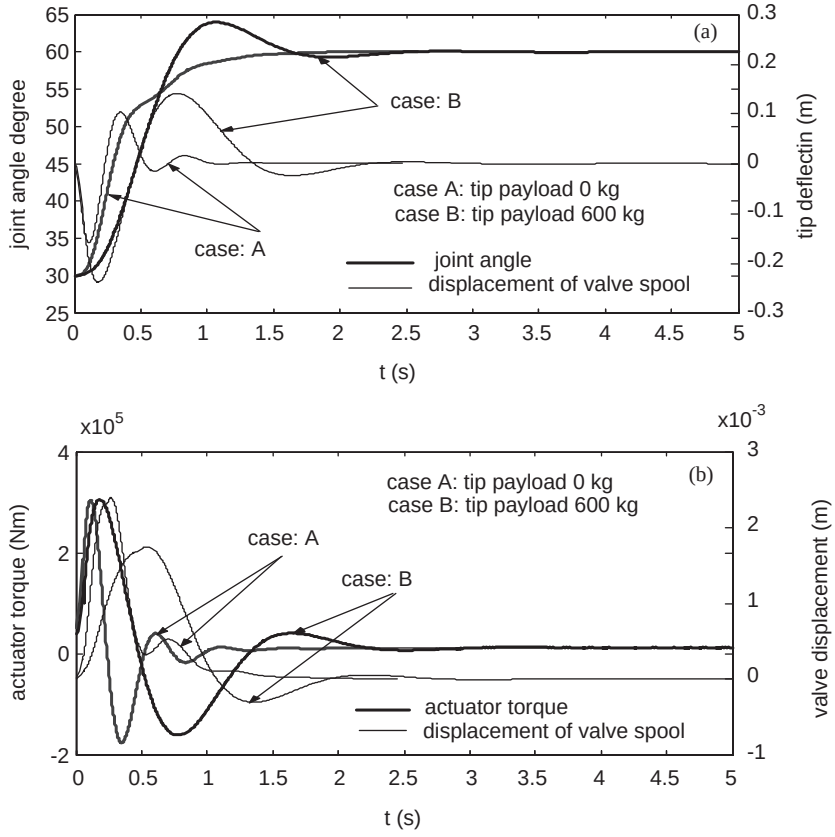

Fig. 6. Simulation results with different tip payloads. (a) Joint angle and tip deflection, (b) torque and displacement of valve spool.

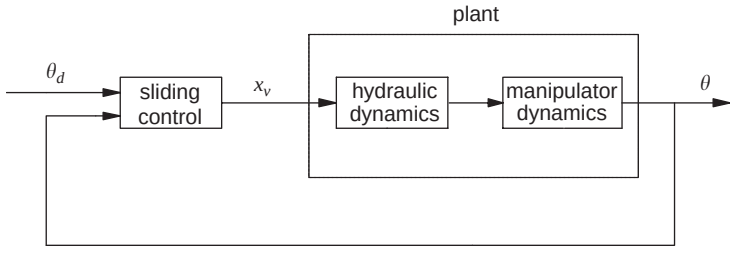

Fig. 7. General structure of direct sliding mode controller.

4.3. Comparison with direct sliding mode control

To compare the performance of the proposed controller with conventional sliding mode controllers used in hydraulic systems e.g. Ref. [22], we implement a sliding mode controller to regulate both the rigid body and flexural vibration of the arm. Fig. 7 shows the general structure

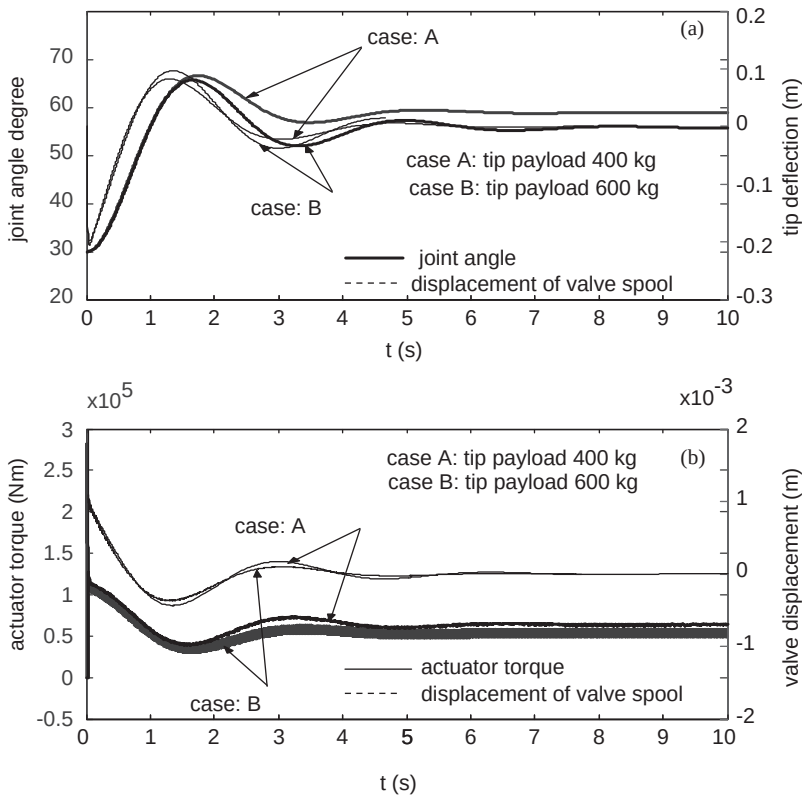

Fig. 8. Simulation results using direct sliding mode controller, and different tip payloads. (a) Joint angle and tip deflection, (b) torque and displacement of valve spool.

of this controller where the output of the sliding mode controller is the spool displacement. Using a saturation function the same as Eq. (47) to reduce chatter in the spool displacement, and similar parameters used in Fig. 6, the simulation results are shown in Fig. 8.

Compared to the previous simulation results, it is evident that although both controllers can provide robust control to a hydraulically driven flexible manipulator, the proposed backstepping controller has a better performance (less overshot, less settling time) with no chatter in the hydraulic valve. Chatter has been one of the main issues in utilizing the sliding mode control. It can be overcome by a backstepping augmentation as shown in Fig. 3.

5. Conclusion

In this paper, a robust controller was proposed to regulate a single-link flexible manipulator driven by a hydraulic actuator. The backstepping technique combined with the sliding mode method was used to control both rigid body and flexural vibration of the link. Parameter uncertainties were considered in the development of the controller and simulation results indicated the robustness of the controller. The stability of the controller was shown by using the

Lyapunov method. It was also shown that when the backstepping method was combined with the sliding mode, chatter in the control input was eliminated. This is the most important characteristic of the proposed controller which provides a smooth and noiseless operation of the servo valve. The extension of the approach to multi-link hydraulically driven flexible manipulators is under investigation.

References

[1] W.J. Book, O. Maizza-Neto, D.E. Whitney, Feedback control of two beam, two joint system with distributed flexibility, *Journal of Dynamic Systems, Measurement and Control* 97 (1975) 424–431.

[2] R.H. Cannon, E. Schmitz, Initial experiments on the end point control of a flexible one-link robot, *International Journal of Robotics Research* 3 (1984) 62–75.

[3] T. Fukuda, Flexibility control of elastic robotic arms, *Journal of Robotic Systems* 2 (1885) 73–88.

[4] P.H. Meckl, W.P. Seering, Reducing residual vibration in systems with uncertain resonances, *IEEE Control Systems Magazine* (1988) 73–76.

[5] M. Hyde, W.P. Seering, Inhibiting multiple mode vibration in controlled flexible systems, *Proceedings of the 1991 American Control Conference*, Boston, MA, 1991, pp. 2449–2454.

[6] J.Y.S. Luh, M.W. Walker, R.P. Paul, Resolved motion force control of robot manipulators, *Journal of Dynamic Systems, Measurement and Control* 102 (1982) 126–133.

[7] F. Pfeiffer, A feedforward decoupling concept for the control of elastic robots, *Journal of Robotics Systems* 6 (1989) 407–416.

[8] H. Asada, Z. Ma, H. Tokumaru, Inverse dynamics of flexible robot arms: modeling and computation for trajectory control, *Journal of Dynamic Systems, Measurement and Control* 112 (1990) 177–185.

[9] C.M. Oakley, R.H. Cannon, Initial experiments on the end-point control of a two-link manipulator with a very flexible forearm, *Proceedings of the 1988 American Control Conference*, Atlanta, GA, 1998, pp. 996–1002.

[10] K.S. Yeung, Y.P. Chen, Regulation of a one-link flexible robot arm using sliding-mode technique, *International Journal of Control* 49 (1989) 1965–1978.

[11] E. Kubica, D. Wang, A fuzzy control strategy for a flexible link robot, *IEEE International Conference on Robotics and Automation*, 1993, pp. 236–241.

[12] W. Cheng, J.T. Wen, A neural control for the tracking control of flexible beam, *IEEE International Conference on Neural and Networks*, 1993, pp. 749–754.

[13] M.J. Panza, R.W. Mayne, Mathematical modeling for actuator flexible beam dynamic systems, *Proceedings of the 12th Biennial ASME Conference on Mechanical Vibration and Noise*, Montreal, 1989, pp. 91–98.

[14] M.J. Panza, R.W. Mayne, Hydraulic actuator tuning in the control of a rotating flexible beam mechanism, *Journal of Dynamic Systems, Measurement and Control* 118 (1996) 449–456.

[15] D.S. Kwon, S.M. Babcock, B.L. Burks, Tracking control of the hydraulically actuated flexible manipulator, *IEEE International Conference on Robotics and Automation*, 1995, pp. 2200–2205.

[16] M. Krstic, I. Kanellakopoulos, P. Kokotovic, *Nonlinear and Adaptive Control Design*, Wiley, New York, 1995.

[17] J.E. Shigley, *Simulation of Mechanical Systems: An Introduction*, McGraw-Hill, New York, 1967.

[18] W.T. Thomson, *Theory of Vibration with Applications*, Prentice-Hall, Englewood Cliffs, NJ, 1981.

[19] J. Panza, R.W. Mayne, Theoretical and experimental investigation of hydraulic actuator interaction in the dynamics of a rotating flexible beam, *Journal of Vibration and Acoustics* 116 (1994) 113–119.

[20] H.E. Merritt, *Hydraulic Control System*, Wiley, New York, 1967.

[21] J.-J.E. Slotine, W. Li, *Applied Nonlinear Control*, Prentice-Hall, Englewood Cliffs, NJ, 1991.

[22] Y. Liu, H. Handroos, Technical note: sliding mode control for a class of hydraulic position servo, *Mechatronics* 9 (1999) 111–123.